

Comparison of CRISPR Sequences in Archaea and Bacteria with Eukaryotic microRNAs

Reyhane Ramezani ¹, Mandana Behbahani ^{2*}, Hassan Mohabatkar ², Kimia Sarraf Mamouri ²
and Fatemeh Hejazi ¹¹. Faculty of Nanochemical Engineering, Shiraz University, Shiraz, Iran². Faculty of Biotechnology, Isfahan University, Isfahan, Iran

Abstract

Background: This study explores repetitive Clustered Regularly Interspaced Short Palindromic Repeats (CRISPR) sequences from the archaea *Acidianus sp.* and *Acidianus ambivalens* (*A. ambivalens*), as well as from the bacterium *Yersinia ruckeri* (*Y. ruckeri*). These sequences are compared with human microRNA (miRNA) sequences to investigate potential genetic similarities and disease associations.**Methods:** CRISPR sequences were retrieved from the CRISPR/Cas⁺⁺ database, and human miRNA sequences were obtained from miRBase. Sequence alignments were performed using BLASTn with an E-value threshold of 1e-5 to identify significant similarities. Genes associated with matched human miRNAs were identified through the HGNC and GeneCards databases. Further analyses included comparison with disease-associated miRNAs reported in human and mouse datasets.**Results:** In *Y. ruckeri*, alignments revealed similarities to miRNAs linked with genes such as *FOXO1*, *PTEN*, *PAX7*, and *DOCK3*, which are associated with lung cancer and muscular dystrophies. In *A. ambivalens*, aligned miRNAs corresponded to loci including *CHM13* and *GRCh38*, potentially linked to perimenstrual adenocarcinoma and mild pre-eclampsia. For *Acidianus sp.*, matches were observed with miRNAs associated with genes like *Irak2*, *NOS2*, *STAT1*, and *Numb*, which have been implicated in Psoriatic arthritis, Alzheimer's disease, Hepatocellular carcinoma, and Coronary artery disease.**Conclusion:** CRISPR sequences from these prokaryotes show notable similarities with human miRNAs, suggesting possible indirect links to genes involved in major diseases. These preliminary findings emphasize the need for further investigation into shared sequence motifs and their functional roles in host-pathogen interactions or evolutionary biology.**Keywords:** Adenocarcinoma, Archaea, Bacteria, Biology, CRISPR/Cas9, Liver neoplasms, Muscular dystrophies, Repetitive CRISPR sequences**To cite this article:** Ramezani R, Behbahani M, Mohabatkar H, Sarraf Mamouri K, Hejazi F. Comparison of CRISPR Sequences in Archaea and Bacteria with Eukaryotic microRNAs. Avicenna J Med Biotech 2025;17(4):258-276.

* Corresponding author:
Mandana Behbahani, Ph.D.,
Faculty of Biotechnology, Isfahan
University, Isfahan, Iran
Tel: +98 31 37934327
Fax: +98 31 37932456
E-mail:
ma_behbahani@yahoo.com
Received: 28 Apr 2025
Accepted: 30 Aug 2025

Introduction

Clustered Regularly Interspaced Short Palindromic Repeats (CRISPR) and their associated Cas proteins constitute an adaptive immune system in bacteria and archaea, providing defense against mobile genetic elements such as phages and plasmids ¹⁻⁴. Since their discovery in *Escherichia coli* (*E. coli*) by Ishino *et al* in 1987 ⁵ (Figure 1), CRISPR/Cas systems have collected significant scientific interest due to their configurable functionality and broad applications in genome editing and molecular biology.

Despite extensive research into the classification, structure, and function of CRISPR arrays in prokary-

otes, limited knowledge exists regarding the presence or potential analogs of these systems in eukaryotic microorganisms. The current body of literature has largely overlooked the possibility of CRISPR-like repetitive elements in unicellular eukaryotes, leaving a critical gap in our understanding of their evolutionary and functional relevance ⁶⁻⁹.

This study seeks to address this gap by systematically comparing CRISPR repeat sequences from bacterial and archaeal genomes with sequence elements identified in eukaryotic microorganisms. We hypothesize that specific repetitive motifs or structural analogs may

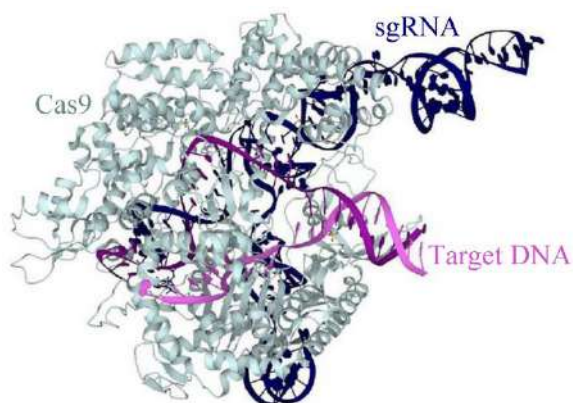


Figure 1. Crystallographic studies have shown that Cas9 consists of two main lobes: a recognition lobe and a nuclease lobe. The binding of guide RNA to target DNA induces the formation of a positively charged groove at the interface of these lobes ¹⁰.

be present in eukaryotic genomes, potentially shedding light on the evolutionary origins of CRISPR-like systems.

To explore this hypothesis, CRISPR sequences were obtained from the CRISPR/Cas⁺ database, while human miRNA sequences were retrieved from the miR-Base repository. Sequence alignments were performed using BLASTn with an E-value threshold of 1e-5 to detect statistically significant similarities. These computational approaches enabled a comparative analysis of sequence features across diverse domains of life, thereby forming the basis for our evolutionary investigation.

A significant advancement in the understanding of CRISPR loci occurred in 1995 when a scientist from the University of Italy identified repetitive DNA structures in the genome of an archaeal organism, revealing similarities to those previously described in bacterial genomes ^{10,11}. This observation led to the early hypothesis that such sequences contain foreign DNA fragments and function as part of an adaptive immune system in both bacteria and archaea ¹²⁻¹⁴. Since then, the CRISPR-Cas system has been increasingly recognized as a powerful defense mechanism and genetic tool. CRISPR loci exhibit a high degree of polymorphism across bacterial strains, including pathogenic species, which has enabled their application in microbial typing and clinical diagnostics. Among the major CRISPR systems, CRISPR-Cas12a is distinguished by its recognition of T-rich PAM sequences, expanding its utility for genome editing in regions inaccessible to CRISPR/Cas9 ¹⁵⁻¹⁷. The CRISPR/Cas9 system itself originates from a natural bacterial defense mechanism. During viral infection, bacteria incorporate short DNA fragments of the invader into their genome, forming CRISPR arrays. These sequences are then transcribed into crRNAs, which guide the Cas9 endonuclease to target and cleave matching sequences in invading DNA, thereby neutralizing the threat ¹⁸⁻²⁰.

CRISPR-Cas systems are categorized into two major classes, six types, and 33 subtypes. Class 1 (types I, III, IV) includes systems with multi-protein effector complexes, while Class 2 (types II, V, VI) contains single multidomain effector proteins such as Cas9, which is characteristic of type II systems found predominantly in bacteria ²¹⁻²⁴. However, the classification of CRISPR-Cas systems is complicated by the emergence of hybrid loci formed through extensive recombination events. These hybrid systems often defy standard classification despite containing canonical Cas genes. Furthermore, multiple CRISPR-Cas systems may coexist within a single genome, and even strains of the same species may carry distinct system types ²⁵.

Many CRISPR-Cas loci are embedded in genomic islands that also encode mobile genetic elements such as transposases, toxin-antitoxin modules, and various defense-related genes. The distribution of CRISPR types is non-uniform among microorganisms: type II systems have been detected only in bacteria, while type III systems are more common in archaea. This pattern is consistent with earlier findings that suggest CRISPR systems are generally more prevalent in archaeal lineages than in bacterial ones ²⁶⁻³⁵.

Despite the promise of CRISPR/Cas9 for antimicrobial applications, one of the significant limitations is the challenge of effective delivery into bacterial cells. While plasmid-based electroporation remains the dominant method for introducing CRISPR components *in vitro*, it is often impractical for *in vivo* use ^{5,36}.

Currently, three primary formats are employed for CRISPR delivery: (1) plasmids encoding both Cas9 and sgRNA, offering a stable DNA-based platform but requiring nuclear entry (Figure 2); (2) RNA-based approaches using sgRNA and mRNA encoding Cas9, which are safer and do not integrate into the host genome; and (3) preassembled Cas9 protein-sgRNA complexes (RNA-AP format), which minimize integra-

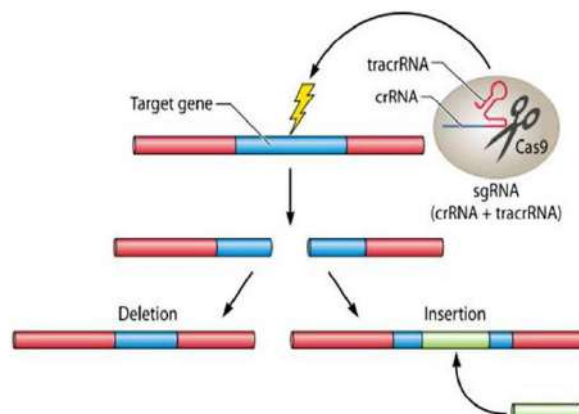


Figure 2. The CRISPR system utilizes a single guide RNA (sgRNA) composed of a target-matching sequence and an activating region that recruits Cas9. This complex precisely induces double-strand breaks at specific genomic sites, leading to gene disruption. Owing to its high accuracy and efficiency, CRISPR is widely adopted in molecular biology and genetic engineering.

CRISPR Sequences in Prokaryotes

Table 1. The three types of transmission for the CRISPR/Cas9 system and their characteristics ⁵

Delivery formats	Delivery payloads	Advantages	Limitations
DNA	CRISPR/Cas9 Plasmid	Most simple and stable	Higher off-target effects, low efficiency
mRNA	Cas9 mRNA and sgRNA	Faster and lower off-target effects	Vulnerable, unstable
Protein	Cas9/sgRNA complex	Rapid and significant reaction off-target effect, toxicity and immune response	Difficult to obtain, Risk of permanent integration into the host

tion risks and can be directly functional (Table 1).

Although the CRISPR-Cas system has been extensively studied for its role in microbial immunity and gene editing, its potential evolutionary or functional relationship with eukaryotic small RNAs such as microRNAs (miRNAs) remains largely unstudied. Therefore, this study aims to investigate the sequence similarities between CRISPR loci in archaea and bacteria and eukaryotic miRNAs, with the objective to uncover potential evolutionary links or functional convergence between these RNA-based regulatory systems.

Materials and Methods

CRISPR/Cas⁺⁺ server

In the present study, the CRISPR/Cas⁺⁺ tool (version 1.1.2, 2021, I2BC) was utilized to extract repetitive sequences from prokaryotic genomes. From a pool of 100 randomly selected prokaryotic species, sequences corresponding to 20 genes and 20 species of bacteria, as well as 20 genera and 20 types of archaea, were retrieved using the miRBase database. These repetitive sequences were subsequently compared with eukaryotic microRNAs obtained from the same database to identify potential sequence similarities. The analysis revealed that only three eukaryotic microRNAs exhibited similarity to the prokaryotic sequences_ specifically, one gene from a bacterial species and one gene from two archaeal species, suggesting a potential role in inter-domain biological communication. It is also noteworthy that some bacterial strains lacked identifiable CRISPR or Cas elements, as reported by the CRISPR/Cas⁺⁺ tool (Table 2).

miRBase server

The key features of miRBase are designed to achieve five main objectives: (1) To establish a standardized naming system for microRNAs; (2) To collect and curate all known microRNA sequences; (3) To provide both human-and machine-readable information for each microRNA; (4) To offer basic supporting evidence for each microRNA (5) and to integrate and provide information regarding microRNA target interactions.

The latest published version (version 22) of miRBase contains information on 38,589 microRNA precursors and 48,860 mature microRNA sequences from 271 different species. Additionally, the database includes 1,493 small RNA sequencing datasets, encompassing more than 5.5 billion reads mapped to microRNAs.

Table 2. Sequences related to bacteria and archaea were obtained using the CRISPR-Cas⁺⁺ server

Archaea	
<i>Acidianus ambivalens</i>	Sequence CP045482.1
<i>Acidianus hospitalis W1</i>	Sequence CP002535.1
<i>Acidianus manzaensis YN-2 5</i>	Sequence CP020477.1
<i>Acidianus sp. HS-5</i>	Sequence AP025245.1
<i>Acidianus sulfidivorans Jp7</i>	Sequence CP029288.2
<i>Acidilobus saccharovorans 345-15</i>	Sequence CP001742.1
<i>Aciduliprofundum boone I</i>	Sequence CP001941.1
<i>Aeropyrum camini SY1</i>	Sequence AP012489.1
<i>Aeropyrum permix K1</i>	Sequence BA000002.3
<i>Archaeoglobus fulgidus DSM</i>	Sequence AE000782.1
<i>Caldisphaera lagunensis DSM 1590 8</i>	Sequence CP003378.1
<i>Methanococcoides methylutens MM1</i>	Sequence CP009518.1
<i>Archaeoglobus sulfatocaldus PM70-1</i>	Sequence CP005290.1
<i>Archaeoglobus veneficus SNP6</i>	Sequence CP002588.1
<i>- Caldisphaera lagunensis</i>	Sequence NR_102472.1
<i>Caldivirga maquilensis IC-167</i>	Sequence CP000852.1
<i>Candidatus Aenigmarchaeota archaeo n</i>	Sequence CP070804.1
<i>Methanococcoides sp. LMO-1</i>	Sequence NZ-CP073710.1
<i>Haloarcula hispanica (euryarchaeotes)</i>	Sequence CP002922.1
<i>archaeon GW2011_AR15</i>	Sequence CP010425.1
Bacteria	
<i>Yersinia pestis (Y. pestis)</i>	Sequence CP064122.2
<i>Y. pestis Pestoides G</i>	Sequence CP010247.1
<i>Y. pestis A1122</i>	Sequence CP009840.1
<i>Y. pestis Pestoides</i>	Sequence CP009715.1
<i>Achromobacter deleyi</i>	Sequence CP065997.1
<i>Zymomonas mobilis subsp. Pomaceae</i>	Sequence CP002866.1
<i>Achromobacter xylosoxidans (b-proteo-bacteria</i>	Sequence CP006818.1
<i>Abssiella argi (firmicutes)</i>	Sequence AP019695.1
<i>Acetobacter aceti (a-proteobacteria)</i>	Sequence AP023326.1
<i>Acetobacter ascendens</i>	Sequence AP023326.1
<i>Y. enterocolitica</i>	Sequence CP009367.1
<i>Yersinia ruckeri (enterobacteria) 17Y015</i>	Sequence CP084649.1
<i>Zymomonas mobilis subsp.</i>	Sequence CP002865.1
<i>Acetobacter aceti NBRC 14818</i>	Sequence AP023410.1
<i>Acanthopleuribacteraceae bacterium</i>	Sequence CP071793.1
<i>Acetobacter aceti</i>	Sequence AP023326.1
<i>Acidovorax carolinensis</i>	Sequence CP021369.1
<i>Acanthopleuribacteraceae bacterium M133</i>	Sequence CP071793.1
<i>Francisella tularensis subsp</i>	Sequence AM233362.1

NCBI server

The National Center for Biotechnology Information (NCBI), part of the National Library of Medicine (NLM), has implemented initial updates to several of

its services to support NIH-funded researchers and institutions in complying with the 2024 NIH Public Access Policy, which took effect on July 1, 2025. As part of this effort, and using tools available on the NCBI platform (version 3.42.0), the similarity index and degree of sequence conservation among repetitive elements from two archaeal species and their related

micro-organisms were analyzed. The comparative analysis results are shown in (Figure 3). Through the use of the NCBI server and by entering the target gene, information regarding its function and the organisms in which it is found was obtained.

HUGO gene server

HUGOgene is a widely used platform for examining

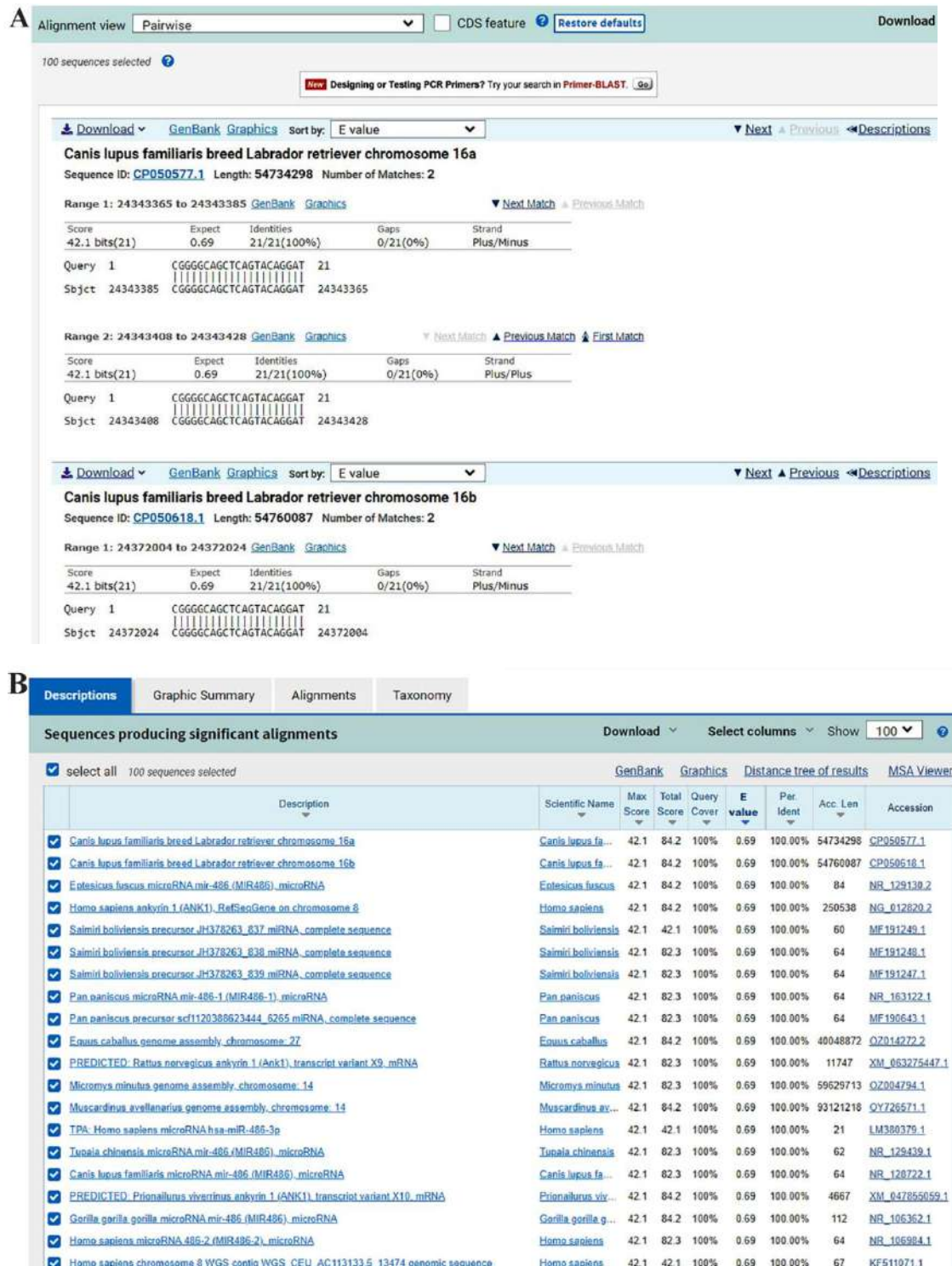


Figure 3. Obtaining the similarities of repetitive sequences in prokaryotes with other organisms, as well as determining the index.

and analyzing genetic variants, genome sequences, and DNA sequence data. Key features of this server include: (1) Genetic data analysis; (2) Variant investigation; (3) Genetic disease diagnosis; (4) Gene and protein identification and characterization.

The HUGO Gene Nomenclature Committee (HGNC) is responsible for assigning a unique and ideally meaningful name and symbol to every human gene. The HGNC database currently contains over 24,000 publicly accessible records, each providing approved gene nomenclature and associated gene information. Recently, the HGNC database was relocated to the European Bioinformatics Institute (EBI). It now offers direct access to various integrated resources, including the searchable HGNC database, the HCOP orthology prediction tool, and manually curated gene family web pages.

In this study, the HUGOgene was used to query a variety of genes and vary their scientifically accepted and officially approved names.

GeneCards server

For over two decades, GeneCards has served as a comprehensive gene-centric database, automatically mining and integrating information from a wide range of data sources. This process results in a web-based card for each of the tens of thousands of human genes. Developed and maintained by the Department of Molecular Genetics at the Weizmann Institute of Science, GeneCards was established in 1997 with the goal of unifying fragmented genetic information from various specialized databases into a coherent and accessible resource. In the present study, utilizing GeneCards at the RNA center, key information regarding the target gene was obtained, including its chromosomal location, exon-intron structure, and potential associations with human diseases.

Results

In this study, the findings focus on three prokaryotic

Table 3. microRNAs accession numbers

Human microRNAs	Accession number
hsa-miR-486-3p	MIMAT0004762
hsa-miR-146a	MIMAT0004
hsa-miR-519e-5p	MIMAT0003145

species: one bacterial and two archaeal. Initially, the repetitive sequences of these species were identified using the CRISPR/Cas system and then compared with repetitive sequences from human microRNAs obtained from the miRBase database. The comparison aimed to identify similarities between bacterial and human microRNAs. Table 3 presents detailed information on several human microRNAs identified during this process. The first column lists the microRNAs, each labeled with the prefix-hsa (Human sapiens), while the second column provides their unique accession numbers from the miRBase database, shown as MIMAT codes, which are essential for accurate identification.

Yersinia ruckeri (*Y. ruckeri*)

Initially, *Yersinia* bacteria were submitted to the CRISPR/Cas⁺⁺ server, where their repetitive sequence were obtained. Following this, human microRNAs similar to the identified sequences were determined using the miRBase server (Figure 4). On the other hand, the multi-gene card server includes genes such as *FOXO1*, *PAX7*, *PTEN*, and *DOCK3*, which are involved in these microRNAs. Additionally, several diseases are associated with these microRNAs, including lung cancer, muscular dystrophy, and Duchenne muscular dystrophy (Table 4 and Figure 5). According to NCBI, sequence IDs are mentioned in supplementary figures S1-S4.

The *FOXO1* gene belongs to the forkhead family of transcription factors, characterized by a conserved forkhead domain. Although its exact function is not yet fully understood, *FOXO1* is believed to play a role in

CUUCACUGCCGCACAGGCAGCUCAGCAGAA

Examples: mature mmu-let-7g hairpin hsa-mir-105-1

Similar sequences

Text search within result Filter Clear Sort by E-value (min to max) - default Hide alignments See details Download

RNA types

☐ pre miRNA (9)

☐ miRNA (2)

Organisms

Homo sapiens (human) microRNA hsa-mir-486 precursor (hsa-mir-486-1)

68 nucleotides

Query 15 AGGCAGCUCAGCUCAG 30

|||||

Sbjct 48 GGCAGCUCAGCUCAG 63

Figure 4. Human miRNAs similar to the *Yersinia ruckeri* bacterial sequence were identified using the miRBase server.

Table 4. Overview of *Yersinia ruckeri* (*Y. ruckeri*) species, their similarity to human genes, and related diseases

<i>Y. ruckeri</i>	CUUCACUGCCG- CACAGGCAGCUCAGAAA			
Homo sapiens (human) hsa-miR-486-3p 21 nucleotides	CGGGGCAGCUCAGUACAGGAU	Query 16 GGCAGCUCAGA 26 	Subject 4 GGCAGCUCAGU 14	
Genes	<i>FOXO1</i>	<i>PTEN</i>	<i>PAX7</i>	<i>DOCK3</i>
Human disease	Lung cancer	Duchenne disease	Muscular dystrophy	
Similarity with other animals	Mouse	Monkey	Horse	Fox

MIR486-1 (MicroRNA 486-1) is an RNA Gene, and is affiliated with the miRNA class. Diseases associated with MIR486-1 include Lung Cancer and Muscular Dystrophy, Duchenne Type. Among its related pathways are Cell differentiation - expanded index and miRs in Muscle Cell Differentiation.

Rfam classification for MIR486-1 Gene

microRNA mir-486 RF00784

Additional gene information for MIR486-1 Gene

Mature hsa-miR-486-5p		Mature hsa-miR-486-3p	
Accession	MIMAT0002177	Accession	MIMAT0004762
Description	Homo sapiens hsa-miR-486-5p mature miRNA	Description	Homo sapiens hsa-miR-486-3p mature miRNA
Sequence	4 - UCCUGUACUGAGCUGCCCGAG - 25	Sequence	46 - CGGGGCAGCUCAGUACAGGAU - 66
Evidence	experimental Illumina [1]	Evidence	experimental Illumina [1]
Database links	RNAcentral TissueAtlas miRBase	Database links	RNAcentral TissueAtlas miRBase
Predicted targets	TargetScan TargetMiner miRDB	Predicted targets	TargetScan TargetMiner miRDB
References			
1. PubMed ID: 17604727 A mammalian microRNA expression atlas based on small RNA library sequencing Landgraf R, Rusu M, Sheridan R, Sewer A, Iovino N, Aravin A, Pfeffer S, Rice A, Kamphorst AO, Landthaler M, Lin C, Soci ND, Hermida L, Fulci V, Chiaretti S, Foa R, Schliwka J, Fuchs U, Novosei A, Muller RU, Schermer B, Bissels U, Imman J, Phan Q, Chien M* *Cell (2007) 129:1401-1414			
2. PubMed ID: 15978578 Identification of human fetal liver miRNAs by a novel method *Fu H, Tie Y, Xu C, Zhang Z, Zhu J, Shi Y, Jiang H, Sun Z, Zheng X*			

Figure 5. Involves retrieving microRNA accession numbers and identifying related human diseases.

the regulation of cellular growth and differentiation. Genetic alterations in this gene have been associated with the development of alveolar rhabdomyosarcoma. In this study, the gene of interest was compared with its mutated variant using the BLAST tool, and the results are illustrated in figure S1. The findings suggest that *FOXO1* may be involved in mitogen-induced growth and differentiation. To further investigate, the gene's FASTA sequence was retrieved and subjected to BLAST analysis, which revealed several mutations linked to human diseases.

A comparative analysis between the wild-type and mutated forms of the gene indicated that approximately 20% of disease-associated mutations in humans are localized within the *FOXO1* gene. These pathogenic mutations were identified using the BLAST+ (version 2.11.0) server, specifically through BLASTn, which was employed throughout this study for similarity searches using the gene's FASTA format.

The *PAX* gene belongs to the transcription factor family and is typically characterized by the presence of a paired box domain, an octapeptide, and a homeodomain. Members of this gene family are known to play critical roles in embryonic development and cancer progression. Although the precise biological function of *PAX7* is not yet fully understood, it is hypothesized to function as a tumor suppressor, particularly due to its fusion with members of the alveolar forkhead family. *PAX7* is believed to contribute to both fetal growth and development and tumorigenesis.

Multiple mutations have been identified within the *PAX7* gene, many of which are associated with human diseases, possibly due to sequence similarities with other genes. According to data retrieved from the NCBI database, comparative analysis between the standard and mutated forms of the gene revealed that approximately 40-60% of the mutations occurring in *PAX7* are pathogenic.

These mutations were identified using the BLAST+ (version 2.11.0) server, with BLASTn format, and the results are presented in figure S2.

PTEN has been widely recognized as a tumor suppressor gene in various types of cancers, primarily due to the function of its encoded protein, which acts as a phosphatidylinositol-4,5-bisphosphate 3-phosphatase. This protein contains a tensin-like domain and a catalytic domain that resembles those found in dual-specificity protein phosphatases. Unlike many protein tyrosine phosphatases, the PTEN protein preferentially dephosphorylates phosphoinositide substrates. By reducing intracellular levels of phosphatidylinositol-4,5-bisphosphate, it negatively regulates key signaling pathways, thereby exerting its tumor suppressor function (Figure S3).

To identify pathogenic mutations, the BLAST server (version 2.11.0+) was used. Throughout this study, BLASTn was employed for all sequence comparisons. Similarity searches were conducted using the FASTA format of the *PTEN* gene.

DOCK3 is selectively expressed in the central nervous system and encodes a member of the Guanine nucleotide Exchange Factor (GEF) family. The encoded protein, also known as cytokine 3, functions both as a regulator of cell adhesion and as a presenilin-binding protein. It facilitates axonal growth within the central nervous system by promoting membrane trafficking and activating G proteins (Figure S4).

Pathogenic mutations in this gene were identified using the BLAST server (version 2.11.0+). Throughout this study, BLASTn was utilized for all sequence analyses. Similarity searches were conducted using the FASTA format of the *DOCK3* gene.

Acidianus ambivalens (*A. ambivalens*)

In the first instance, by inputting *A. ambivalens* into the CRISPR/Cas⁺⁺ server, its repeated sequence was obtained. After obtaining the repeated sequence of *A. ambivalens*, using the miRBase server, human microRNAs similar to the mentioned sequences were identified.

According to the multi-gene card server, the *GRCH38* and *CHM13* genes are involved in these microRNAs, and four types of diseases can also be associated with these microRNAs. Such as adenocarcinoma of lung, thyroid neoplasms, stomach neoplasms and, uterine cervical neoplasms, which are related to these microRNAs, were identified (Table 5). According to NCBI, sequence IDs are listed in supplementary

figures S5-S7.

The *CFH* gene, as annotated in the CHM13 genome, encodes a secreted protein that belongs to the complement factor H protein family. This protein interacts with *Pseudomonas aeruginosa* elongation factor Thf, in conjunction with plasminogen, which subsequently undergoes proteolytic activation. It has been proposed that Tuf functions as a virulence factor by recruiting host proteins to the bacterial surface, thereby modulating complement activity and facilitating tissue invasion. Mutations in the *CFH* gene have been associated with an increased risk of atypical Hemolytic-Uremic Syndrome (aHUS) [RefSeq, Oct 2009].

To identify pathogenic mutations, the BLAST+ v2.11.0 server was used, with BLASTn employed for the analysis. Similarity searches were conducted using the FASTA format of the *CFH* gene sequence. The results are illustrated in figure S6.

The *TP53* gene, as annotated in the GRCh/hg38 reference genome, encodes a tumor suppressor protein that contains transcriptional activation, DNA-binding, and oligomerization domains. This protein plays a critical role in responding to various cellular stress signals by regulating the expression of target genes involved in cycle arrest, apoptosis, senescence, DNA repair, and metabolic processes.

Mutations in *TP53* are associated with numerous human cancers, including hereditary cancer syndromes such as Li-Fraumeni syndrome. Alternative splicing events and the use of alternate promoters result in multiple transcript variants and protein isoforms. Furthermore, additional isoforms may arise from the use of alternative translation initiation codons within the same transcript variants (PMIDs: 12032546, 20937277) [RefSeq, Dec 2016].

This gene has also been reported to be associated with the microRNA as mentioned above. To identify potential pathogenic mutations, the BLAST+ v2.11.0 server was used, employing the BLASTn algorithm throughout the study. Sequence similarity searches were performed using the FASTA format of the *TP53* gene. The results are presented in figure S7.

Acidianus S.P

Initially, the sequence of archaea was obtained by inputting it into the CRISPR/Cas⁺⁺ server. These microRNAs are linked to several human diseases, including rheumatoid arthritis, Alzheimer's disease, thyroid cancer, and carcinoma. Using the GeneCards server,

Table 5. Summary of *Acidianus ambivalens* (*A. ambivalens*), similarity to human microorganisms, genes involved in this microorganism, and associated diseases

<i>A. ambivalens</i>	GTTGCATCCCAAAGGGATTGAAAG	
Homo sapiens (human) hsa-miR-519e-5p 22 nucleotides	UUCUCCAAAAGGGAGCACUUUC	Query 9 CCAAAAGGGA 18 Subject 5 CCAAAAGGGA 14
Genes	<i>GRCH38</i>	<i>CHM13</i>
Diseases in human	Adenocarcinoma of lung Stomach neoplasms	Thyroid neoplasms Uterine cervical neoplasms

Table 6. A summary of archaea repetitive sequences, their similarity to human microRNAs, the genes associated with these microRNAs, and the related diseases is provided

<i>Acidianus</i> sp. (<i>cernarchaeotes</i>)	CTTTCAGTTCTTCCTTATTCA	
Homo sapiens (human) hsa-miR-146a-3p	CCUCUGAAAUUCAGUUCUUA	Query 1 CCUCUGAAAUUCAGUUC 17 Subject 1 CCUCUGAAAUUCAGUUC 17
Genes	<i>Irak2, Ifng, NOS2, Hipk3, Numb, STAT1</i>	
Diseases associated with human	Psoriatic arthritis/Rheumatoid arthritis/Alzheimer's disease/Hepatocellular carcinoma/Thyroid cancer/Endogenous coronary artery disease	
Mouse-related diseases	Endocrine and exocrine glands/Disturbance in growth and body size/Homeostasis and metabolism/Cell death (senescence)	

the genes involved in these microRNAs and the diseases associated with them were identified. According to the results, the server highlighted the following genes: *Irak2*, *NOS2*, *Hipk3*, *Numb*, and *STAT1*. Further details are provided below.

Psoriatic arthritis is a disease characterized by joint inflammation (arthritis) that is often associated with a skin condition called psoriasis. It is a chronic inflammatory disease marked by patches of red, irritated skin, usually covered with scaly, white crusts. People with this condition may also experience changes in their fingernails and toenails, such as pitting, thickening, crumbling, or separation from the nail bed.

Rheumatoid arthritis is an autoimmune disorder characterized by pain, swelling, stiffness, and joint damage. While it can affect any joint, it most commonly impacts the wrists and fingers. This condition is more prevalent in women than men and typically onset in middle age. Rheumatoid arthritis development is influenced by a combination of genetic factors, environmental triggers, and hormonal changes. Treatment strategies include pharmacological interventions, lifestyle modifications, and surgical options, all of which aim to alleviate symptoms, reduce pain and swelling, and slow disease progression.

Non-medullary thyroid cancer refers to malignancies originating from follicular cells, which represent more than 95% of all thyroid cancer cases. Cancers arising from parafollicular cells are comparatively rare. Hepatocellular carcinoma is the most prevalent form of primary malignant liver tumor, ranking as the fifth most common cancer globally and the third leading cause of cancer-related mortality. The primary risk factors for hepatocellular carcinoma include chronic infection with hepatitis B or C viruses, prolonged exposure to aflatoxin-contaminated food, and excessive alcohol consumption. Hepatoblastoma, which constitutes 1-2% of pediatric malignant neoplasms, predominantly affects children under the age of three (Table 6) (Figures 6 and 7). According to NCBI, sequence IDs were mentioned in supplementary figures S8-S13.

STAT1 functions as a key activator within various signaling pathways and is encoded by the *STAT1* gene. This protein is activated by interferons α and γ , as well as by Epidermal Growth Factor (EGF). STAT1 plays a crucial role in the immune response against a range of pathogens, including viruses, fungi, and mycobacteria, and is also involved in signaling responses to cytokines and growth factors. Upon activation, STAT1 undergoes phosphorylation, resulting in the formation of homo- or

Jump to section	Aliases	Disorders	Domains	Drugs	Expression	Function	Genomics	Localization	Orthologs
	Paralogs	Pathways	Products	Proteins	Publications	Sources	Summaries	Transcripts	Variants
Research Products	Antibodies	Assays	Proteins	Inhib. RNA	CRISPR	miRNA	Drugs	Cell Lines	Clones
<p>UC009T399848, UC009T399912, UC009T399958, UC009T399970</p> <p>Search aliases for MIR146A gene in PubMed and other databases</p> <p>Summaries for MIR146A Gene</p> <p>NCBI Gene Summary for MIR146A Gene</p> <p>microRNAs (miRNAs) are short (20-24 nt) non-coding RNAs that are involved in post-transcriptional regulation of gene expression in multicellular organisms by affecting both the stability and translation of mRNAs. miRNAs are transcribed by RNA polymerase II as part of capped and polyadenylated primary transcripts (pri-miRNAs) that can be either protein-coding or non-coding. The primary transcript is cleaved by the Drosha ribonuclease III enzyme to produce an approximately 70-nt stem-loop precursor miRNA (pre-miRNA), which is further cleaved by the cytoplasmic Dicer ribonuclease to generate the mature miRNA and antisense miRNA star (miRNA*) products. The mature miRNA is incorporated into a RNA-induced silencing complex (RISC), which recognizes target mRNAs through imperfect base pairing with the miRNA and most commonly results in translational inhibition or destabilization of the target mRNA. Some of the targets of the encoded miRNA are the transcripts for tumor necrosis factor, interleukin 1 receptor-associated kinase 1, interleukin 1-beta, TNF receptor-associated factor 6, and complement factor H. The RefSeq represents the predicted microRNA stem-loop. [provided by RefSeq, Sep 2015]</p> <p>GeneCards Summary for MIR146A Gene</p> <p>MIR146A (MicroRNA 146a) is an RNA Gene, and is affiliated with the miRNA class. Diseases associated with MIR146A include Psoriatic Arthritis and Alzheimer's Disease. Among its related pathways are Toll-like receptor signaling pathway and ApoE and miR-146 in inflammation and atherosclerosis.</p> <p>Gene Wiki entry for MIR146A Gene</p> <p>Additional gene information for MIR146A Gene</p> <p>HGNC (31533) NCBI Gene (406938) Ensembl (ENSG00000283733) OMIM® (610566) Open Targets Platform(ENSG00000283733)</p> <p>Monarch Initiative Alliance of Genome Resources</p> <p>Search for MIR146A at DataMed Search for MIR146A at HumanCyc</p> <p>No data available for CIVIC Summary, UniProtKB/Swiss-Prot Summary, Tocris Summary, PharmGKB Summary, Rfam classification and piRNA Summary for MIR146A Gene</p>									

Figure 6. A summary of has-miR146a is provided, along with supporting evidence and its corresponding accession number.

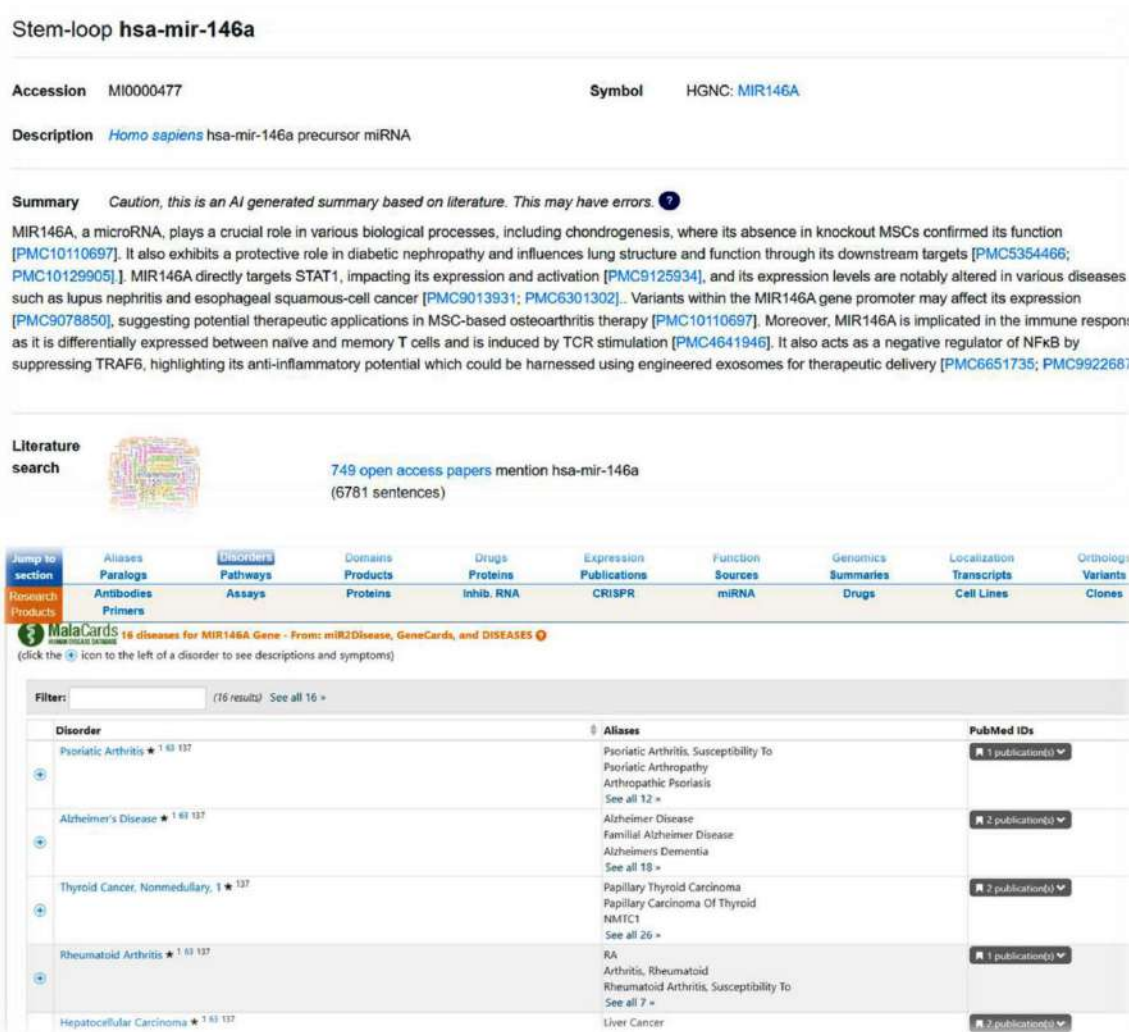


Figure 7. Several human diseases are associated with this microRNA, according to data from the GeneCards database.

heterodimers, often involving other STAT family members and associated kinases (Figure S8).

To identify pathogenic mutations, the BLAST+ v2.11.0 server was used, with the BLASTn algorithm applied throughout the study. Similarity searches were conducted using the FASTA sequence format of the *STAT1* gene.

The protein *Irak2* encoded by this gene belongs to the STAT1 protein family, which, in response to cytokines and growth factors, undergoes phosphorylation by receptor-associated kinases. These phosphorylated proteins subsequently form stable homo- or heterodimers, which are translocated to the cell nucleus, where they function as transcriptional activators. The encoded protein can be activated by a variety of ligands, including interferons alpha and gamma, interleukin-6, EGF, and Platelet-Derived Growth Factor (PDGF). This protein plays a critical role in regulating the expression of genes essential for cell survival in response to various cellular stimuli and pathogens, and it is vital in mediating immune responses to infections caused by patho-

gens, viruses, and mycobacteria. Mutations in this gene have been linked to immunodeficiency (Figure S9). To identify pathogenic mutations, the BLAST+ v2.11.0 server was used, with the BLASTn algorithm applied throughout the study. Similarity searches were conducted using the FASTA sequence format of the *Irak2* gene.

NOTCH1 encodes a protein that is a member of a family of membrane-bound proteins, characterized by structural features such as an extracellular domain composed of multiple EGF repeats and an intracellular domain containing several distinct domain types. This gene is a key component of an evolutionarily conserved intercellular signaling pathway that governs the interactions between neighboring cells (Figure S10). Pathogenic mutations were identified using the BLAST server (BLAST+ version 2.11.0). All analyses in this study were conducted using the BLASTn algorithm. Similarity searches were performed based on the FASTA format of the target gene.

Table 7. BLAST-based analysis showing sequence identity, coverage, and E-values for bacterial and archaeal species aligned with the target gene

<i>Bacteria/Archaeobacteria</i>	Per. Identity	Query cover	E-value
<i>Acidianus s.p</i>	100%	100%	1e-5
<i>Yersinia ruckeri</i>	99%	96%	1e-5
<i>Acidianus ambivalens</i>	100%	84%	1e-5

Nitric oxide, also known as NOS₂, is an active free radical that serves as a biological mediator in various physiological processes, including neurotransmission, antimicrobial defense, and antitumor activity. This gene encodes a nitric oxide synthase enzyme that is primarily expressed in the liver and is upregulated by lipopolysaccharides and specific cytokines (Figure S11). Pathogenic mutations were identified using the BLAST server (BLAST+ version 2.11.0). The BLASTn algorithm was employed throughout the study. Sequence similarity searches were conducted using the FASTA format of the gene.

The *Hipk3* gene activates serine/threonine kinase activity and negatively regulates the kinase. By analyzing the sequence of the healthy gene and comparing it with the defective one, it was determined that nearly 30% of the mutations occurred in the faulty gene (Figure S12). Pathogenic mutations were identified through analyses performed on the BLAST server (BLAST+ v2.11.0). All similarity searches in this study utilized the BLASTn algorithm, with queries conducted using the FASTA format of the target gene.

The final gene, *Numb*, is involved in the regulation of cell fate determination during development. The protein encoded by this gene undergoes degradation in a proteasome-dependent manner, facilitated by a membrane-bound protein (Figure S13). Pathogenic mutations were identified using the BLAST server (BLAST+ v2.11.0), with all analyses conducted using the BLASTn algorithm. Sequence similarity searches were performed based on the gene's FASTA-formatted sequence.

Finally, the E-values (set to 1e-5), identity percentages, and query coverage provided by the respective servers support the purported sequence similarities (Table 7).

Discussion

About ten years ago, the emergence of CRISPR marked a significant turning point in the field of genome editing, suggesting a more precise and cost-effective alternative to earlier methods. By studying and engineering Cas enzymes derived from different bacterial species, the technology rapidly advanced, gaining impressive versatility in a relatively short time. This quick evolution has accelerated scientific research, allowing researchers worldwide to investigate a wide range of biological processes with greater accuracy and depth.

Despite its many benefits, CRISPR also presents several challenges, including variable editing efficiency, reliance on clonal selection, and the risk of off-target effects. These issues are particularly relevant in cancer research, where tumor heterogeneity complicates the isolation of CRISPR-modified clones. Cells with different drug responses or stages of differentiation may be lost during selection, making it challenging to generate models that accurately reflect the complexity of the original tumor.

Even so, CRISPR has already established itself as an invaluable tool for studying the molecular basis of cancer and for dissecting the interactions between specific pathways and genes. So, it is expected to play an increasingly important role in both basic and translational research. Further studies will likely refine CRISPR's utility in probing *in vivo* biological mechanisms using more advanced, clinically relevant models. Additionally, its applications are expected to expand in areas such as adoptive cell therapies, which are becoming central to both cancer treatment and the management of degenerative diseases³⁵.

It is critical to emphasize that the findings of this study are based on computational analyses using public databases and sequence alignment tools. Although these *in silico* approaches can provide valuable preliminary insights into the possible similarities between CRISPR loci and human microRNAs, they are no substitute for laboratory confirmation. Experimental validation or functional tests are necessary to confirm the biological significance and functional implications of these observed similarities. Without such validation, the results should be interpreted with caution, as they may be affected by the quality of the databases or the algorithmic limitations of BLAST and other bioinformatics tools. Therefore, future studies should incorporate laboratory-based experiments to substantiate the computational predictions of this study and increase the robustness of the results.

Given that some of these sequences align with human microRNAs and are associated with mutations in disease-related genes, this area of research holds considerable promise. It raises crucial questions about cross-domain interactions and warrants further investigations to understand its implications for human health better.

Conclusion

Given the complexity and highly dynamic evolution

CRISPR Sequences in Prokaryotes

Table 8. Summary of the examined bacterial names, their repetitive sequences, corresponding microRNA sequences, and their similarity using CRISPR/Cas⁺⁺, miRBase, and BLAST sites

Bactria/Archaea	CRISPR Sequences	microRNA	BLAST
<i>Yersinia ruckeri</i> (<i>enterobacteria</i>)	CTTCACTGCCG- CACAGGCAGCTCAGAAA	Homo sapiens hsa-miR-486-3p 21 nucleotides	Query 16 GGCAGCUCAGA 26 Subject 4 GGCAGCUCAGU 14
<i>Acidianus</i> <i>sp.(crenarchaeote)</i>	CTTTCAGTTCTTCCTTATTTCAA	Homo sapiens hsa-miR-146-3P 22 nucleotides	Query 1 CCUCUGAAAUUCAGUUC 17 Subject 1 CCUCUGAAAUUCAGUUC 17
<i>Acidianus</i> <i>ambivalens</i>	GTTGCATCCCAAAGGGATTGAAAG	Homo sapiens hsa-miR-519e-5p 22 nucleotides	Query 9 CCAAAAGGGA 18 Subject 5 CCAAAAGGGA 14
Human-related diseases		Involved genes	Bacteria, Archaea
Lung cancer, muscular dystrophy, and Duchenne disease		<i>FOXO1, PTEN, PAX7, DOCK3</i>	<i>Yersinia ruckeri</i>
Mild peri-eclampsia, periemboic adenocarcinoma		<i>CHM13, GRCH38</i>	<i>Acidianus ambivalens</i>
psoriatic arthritis, rheumatoid arthritis, Alzheimer's disease, thyroid cancer, liver cancer, and Endocrine Comer's disease		<i>Irak2, NOS2, Hipk3, STAT1</i>	<i>Acidianus s.p</i>

of CRISPR/Cas9 systems, attempting to classify them based on a single criterion—such as the phylogenetic analysis of Cas1—would be inadequate and potentially misleading. A comprehensive classification requires consideration of multiple factors to reflect the diversity and functional variability of these systems accurately. In this study, the repetitive sequence of *Y. ruckeri* and two different species of archaeobacterium, *Acidianus*, were obtained using the CRISPR/Cas9 system. Similar microRNAs from humans and animals, as identified on the miRBase site, were then compared with these sequences, and the degree of similarity with microRNAs was determined. In the continuation of the research, genes involved in bacteria and archaea were obtained using NCBI servers and GeneCards. Moreover, the diseases associated with human microRNAs similar to the bacterial and archaeal repetitive sequences were identified using the RNACenter section of the GeneCards server ³⁶. Table 8 summarizes the relevant results.

Acknowledgement

The authors thank the Department of Biotechnology, Faculty of Advanced Sciences and Technologies, University of Isfahan, for supporting this study.

This work should be attributed to the Faculty of Biotechnology, Isfahan University, Isfahan, Iran

Conflict of Interest

The authors declared no conflict of interest related to this article.

Funding: This work should be attributed to the Faculty of Biotechnology, Isfahan University, Isfahan, Iran.

References

- Raghuram A, Banskota S, Liu DR. Therapeutic in vivo delivery of gene editing agents. *Cell* 2022;185(15):2806-27.
- Taha EA, Lee J, Hotta A. Delivery of CRISPR-Cas tools for in vivo genome editing therapy: Trends and challenges. *J Control Release* 2022;342:345-61.
- Li T, Yang Y, Qi H, Cui W, Zhang L, Fu X, et al. CRISPR/Cas9 therapeutics: progress and prospects. *Signal Transduct Target Ther* 2023;8(1):36.
- Ishibashi R, Maki R, Toyoshima F. Gene targeting in adult organs using in vivo cleavable donor plasmids for CRISPR-Cas9 and CRISPR-Cas12a. *Sci Rep* 2024;14(1):7615.
- Ishino Y, Shinagawa H, Makino K, Amemura M, Nakata A. Nucleotide sequence of the *iap* gene, responsible for alkaline phosphatase isozyme conversion in *Escherichia coli*, and identification of the gene product. *J Bacteriol* 1987;169(12):5429-33.
- Adli M. The CRISPR tool kit for genome editing and beyond. *Nat Commun* 2018;9(1):1911.
- González F, Zhu Z, Shi ZD, Lelli K, Verma N, Li QV, et al. An iCRISPR platform for rapid, multiplexable, and inducible genome editing in human pluripotent stem cells. *Cell Stem Cell* 2014;15(2):215-26.
- Zhang XH, Tee LY, Wang XG, Huang QS, Yang SH. Off-target effects in CRISPR/Cas9-mediated genome engineering. *Mol Ther Nucleic Acids* 2015 Nov 17;4(11):e264.
- Weisheit I, Kroeger JA, Malik R, Klimmt J, Crusius D, Dannert A, et al. Detection of deleterious on-target effects after HDR-mediated CRISPR editing. *Cell Rep* 2020;31(8):107689.
- Nishimasu H, Ran FA, Hsu PD, Konermann S, Shehata SI, Dohmae N, et al. Crystal structure of Cas9 in complex with guide RNA and target DNA. *Cell* 2014;156(5):935-49.
- Höijer I, Emmanouilidou A, Östlund R, Van Schendel R, Bozorgpana S, Tijsterman M, et al. CRISPR-Cas9 induces large structural variants at on-target and off-target sites in vivo that segregate across generations. *Nat Commun* 2022;13(1):627.

12. Zetsche B, Gootenberg JS, Abudayyeh OO, Slaymaker IM, Makarova KS, Essletzbichler P, et al. Cpf1 is a single RNA-guided endonuclease of a class 2 CRISPR-Cas system. *Cell* 2015;163(3):759-71.
13. Mojica FJ, Díez-Villaseñor CS, García-Martínez J, Soria E. Intervening sequences of regularly spaced prokaryotic repeats derive from foreign genetic elements. *J Mol Evol* 2005;60(2):174-82.
14. Bolotin A, Quinquis B, Sorokin A, Ehrlich SD. Clustered regularly interspaced short palindrome repeats (CRISPRs) have spacers of extrachromosomal origin. *Microbiology (Reading)* 2005;151(Pt 8):2551-61.
15. Krysler AR, Cromwell CR, Tu T, Jovel J, Hubbard BP. Guide RNAs containing universal bases enable Cas9/Cas12a recognition of polymorphic sequences. *Nat Commun* 2022;13(1):1617.
16. Hirsch F, Iphofen R, Koporc Z. Ethics assessment in research proposals adopting CRISPR technology. *Biochem Med (Zagreb)* 2019;29(2):020202.
17. Cai L, Zheng LA, He L. The forty years of medical genetics in China. *J Genet Genomics* 2018;45(11):569-82.
18. Memi F, Ntokou A, Papangeli I. CRISPR/Cas9 gene-editing: Research technologies, clinical applications, and ethical considerations. *Semin Perinatol* 2018;42(8):487-500.
19. Hundleby PA, Harwood WA. Impacts of the EU GMO regulatory framework for plant genome editing. *Food Energy Secur* 2019;8(2):e00161.
20. Rodriguez E. Ethical issues in genome editing using CRISPR/Cas9 system. *Journal of Clinical Research and Bioethics* 2016;7(2).
21. Esvelt KM, Smidler AL, Catteruccia F, Church GM. Concerning RNA-guided gene drives for the alteration of wild populations. *Elife* 2014;3:e03401.
22. Shinwari ZK, Tanveer F, Khalil AT. Ethical issues regarding CRISPR-mediated genome editing. *Curr Issues Mol Biol* 2018;26(1):103-10.
23. Makarova KS, Grishin NV, Shabalina SA, Wolf YI, Koonin EV. A putative RNA-interference-based immune system in prokaryotes: computational analysis of the predicted enzymatic machinery, functional analogies with eukaryotic RNAi, and hypothetical mechanisms of action. *Biol Direct* 2006;1:1-26.
24. Carthew RW, Sontheimer EJ. Origins and mechanisms of miRNAs and siRNAs. *Cell* 2009;136(4):642-55.
25. Barrangou R, Fremaux C, Deveau H, Richards M, Boyaval P, Moineau S, et al. CRISPR provides acquired resistance against viruses in prokaryotes. *Science* 2007;315(5819):1709-12.
26. Garrett RA, Shah SA, Vestergaard G, Deng L, Gudbergdottir S, Kenchappa CS, et al. CRISPR-based immune systems of the Sulfolobales: complexity and diversity. *Biochem Soc Tran* 2011;39(1):51-7.
27. Garneau JE, Dupuis MÈ, Villion M, Romero DA, Barrangou R, Boyaval P, et al. The CRISPR/Cas bacterial immune system cleaves bacteriophage and plasmid DNA. *Nature* 2010;468(7320):67-71.
28. Sontheimer EJ, Marraffini LA. Slicer for DNA. *Nature* 2010;468(7320):45-6.
29. Mojica FJ, Díez-Villaseñor C, García-Martínez J, Almendros C. Short motif sequences determine the targets of the prokaryotic CRISPR defense system. *Microbiology (Reading)* 2009;155(3):733-40.
30. Deveau H, Barrangou R, Garneau JE, Labonté J, Fremaux C, Boyaval P, et al. Phage response to CRISPR-encoded resistance in *Streptococcus thermophilus*. *J Bacteriol* 2008;190(4):1390-400.
31. Brouns SJ, Jore MM, Lundgren M, Westra ER, Slijkhuys RJ, Snijders AP, et al. Small CRISPR RNAs guide antiviral defense in prokaryotes. *Science* 2008;321(5891):960-4.
32. Deltcheva E, Chylinski K, Sharma CM, Gonzales K, Chao Y, Pirzada ZA, et al. CRISPR RNA maturation by trans-encoded small RNA and host factor RNase III. *Nature* 2011;471(7340):602-7.
33. Haurwitz RE, Jinek M, Wiedenheft B, Zhou K, Doudna JA. Sequence- and structure-specific RNA processing by a CRISPR endonuclease. *Science* 2010;329(5997):1355-8.
34. Lyu C, Shen J, Wang R, Gu H, Zhang J, Xue F, et al. Targeted genome engineering in human induced pluripotent stem cells from patients with hemophilia B using the CRISPR-Cas9 system. *Stem Cell Research & Therapy* 2018;9:1-12.
35. Yin H, Song CQ, Suresh S, Wu Q, Walsh S, Rhym LH, et al. Structure-guided chemical modification of guide RNA enables potent non-viral in vivo genome editing. *Nature biotechnology* 2017;35(12):1179-1187.
36. Frangoul H, Altshuler D, Cappellini MD, Chen YS, Domm J, Eustace BK, et al. CRISPR-Cas9 gene editing for sickle cell disease and β -thalassemia. *New England Journal of Medicine* 2021;384(3):252-260.

CRISPR Sequences in Prokaryotes

Query	352	CCCCCTCCCGTCGCGCCCCAGTGTCTGCTTCTCCCCCTCTTGCTCTCTCTCGGGCTggg	411
Sbjct	371	CCCCCTCCCCCTCGCGCCCCAGTGTCTGCTTCTCTCCCTCTTGCTCTCTCTCGGGCTGGG	430
Query	412	ggggggggggggggTACCATTGGCGAGGGCGCTCAGTGGTGGAGATCAACCCGGACTTC	471
Sbjct	431	GGAGGGGGGGGGGTACCATTGGCGAGGGCGCTCAGTGGTGGAGATCAACCCGGACTTC	490
Query	472	GAGCGCTGCCCGGCGCGCTCTGTGCACCTGGCGCTGCCAGGCGGAGTTTAGCCAG	531
Sbjct	491	GAGCGCTGCCCGGCGCGCTCTGTGCACCTGGCGCTGCCAGGCGGAGTTTAGCCAG	550
Query	532	TCCAACCTGGCAACCTCCAGCCCGGCGCGTCTGGGACGCGCGGCTGCCAACCCGACGCC	591
Sbjct	551	TCCAACCTGGCAACCTCCAGCCCGGCGCGTCTGGGACGCGCGGCTGCCAACCCGACGCC	610
Query	592	GCGGCGGGCTGCCCTCGGCTCTGGCTGCCGCTGTCAAGCGCCGACTTCATGAGCAACTG	651
Sbjct	611	GCGGACAGGCTGCCCTCGGCTCTGGCTGCCGCTGTCAAGCGCGACTTCATGAGCAACTG	670
Query	652	AGCTTGCTGGAGGAGAGCAGGACTTCCCGCAGcgccccggctccggcgccggcgggg	711
Sbjct	671	AGCTTGCTGGAGGAGAGCAGGACTTCCCGCAGCGCCCGGCTCCGTGGCGCGCGCGGTG	730
Query	712	ggcgggcgccggcgccccggcgcccgccacccggggggcggtgccccgggACTTCAGGGCCCGGAG	771
Sbjct	731	GCGGCGCGGGCGGCGCGCGGCGGCACCGGGGGGCTGTGCGGGGACTTCAGGGCCCGGAG	790
Query	772	CGGGGCTGCTTgcaccacagcgccaccgcagccccggcgccccggcgccgtgtcgcagcac	831
Sbjct	791	CGGGGCTGCTTGACCCAGCGCCACCGCAGCCCCCGCGCCCGGGGCGCTGTTCGAGCAC	850
Query	832	ccggcggtgccccccggcgccgctggggcggtccggGGGGCAGCGCGCAAGAGCAGCTCG	891
Sbjct	851	CGCGCAGTGCAACCGCGCGCCC---GGGCGCTCTCGGGGCGAGCGCGCAAGAGCAGCTCG	907
Query	892	TCCCGCGCAACCGGTGGGCGAACTGTCTACGCCAGCTCATCACCAAGCGCATCGAG	951
Sbjct	908	TCCCGCGCAACCGGTGGGCGAACTGTCTACGCTGATCTCATCACCAAGGCGCATCGAG	967
Query	952	AGCTCGCGGAGAGCGCGCTACGCTGTGCGAGATCTACGAGTGGATGGTCAAGAGCGTG	1011
Sbjct	968	AGCTCGGCGGAGAGCGGCTACGCTGTGCGAGATCTACGAGTGGATGGTCAAGAGCGTG	1027
Query	1012	CCCTACTTCAAGGATAAGGGTGACAGCAACAGCTCGCGGGCTGGAAG	1059
Sbjct	1028	CCCTACTTCAAGGATAAGGGTGACAGCAACAGCTCGCGGGCTGGAAG	1075

Figure S1. BLASTn-based graphical comparison of *FOXO1* gene sequences showing 30% mutation relative to the reference FASTA.

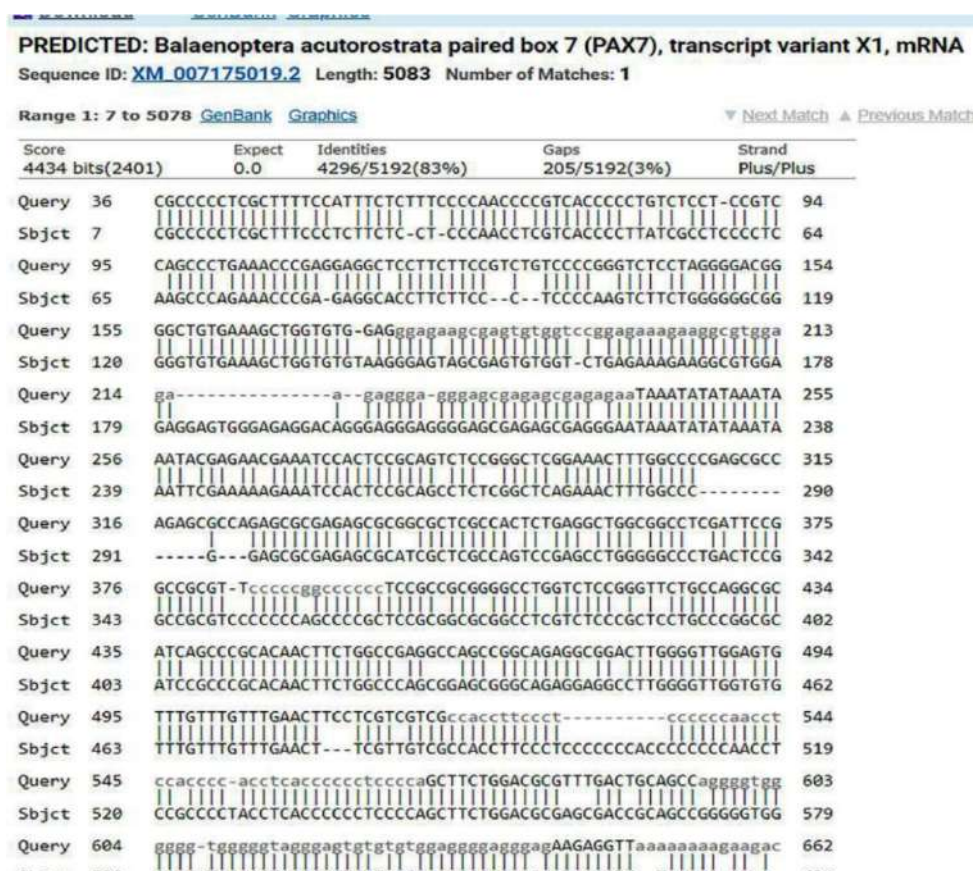


Figure S2. Comparative BLASTn analysis of *PAX7* gene sequences revealed ~30% mutation by aligning the reference FASTA sequence with defective variants, highlighting key sequence similarities and mutation sites.

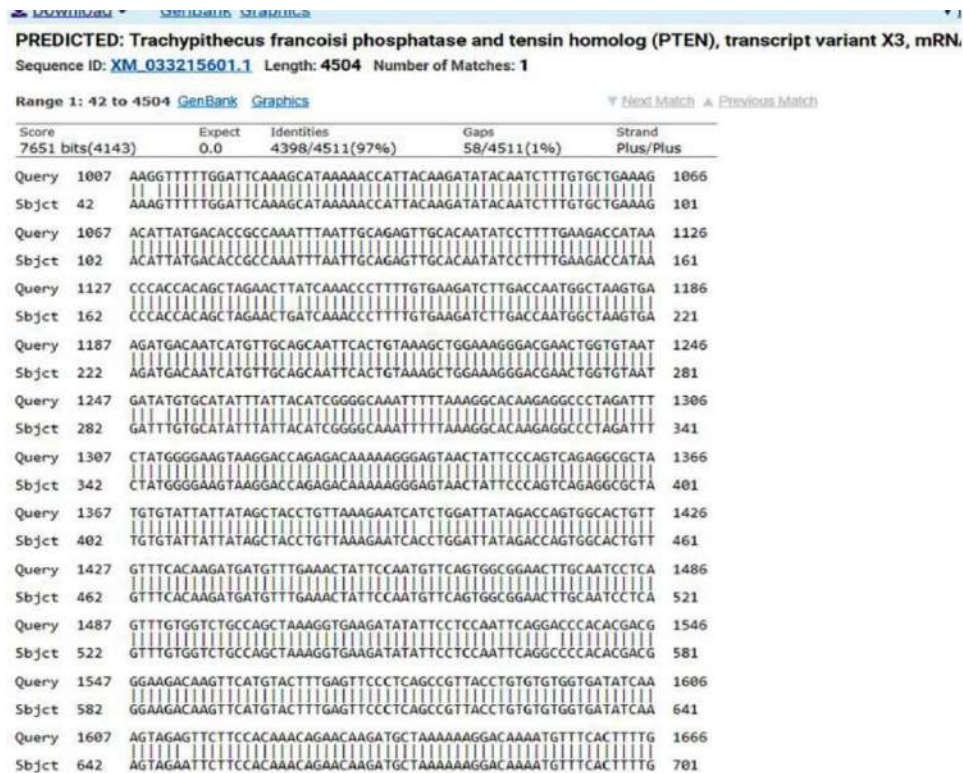


Figure S3. BLASTn-based graphical comparison of *PTEN* gene sequences showed ~30% mutation by aligning defective sequences with the reference FASTA, revealing conserved regions and mutation sites.

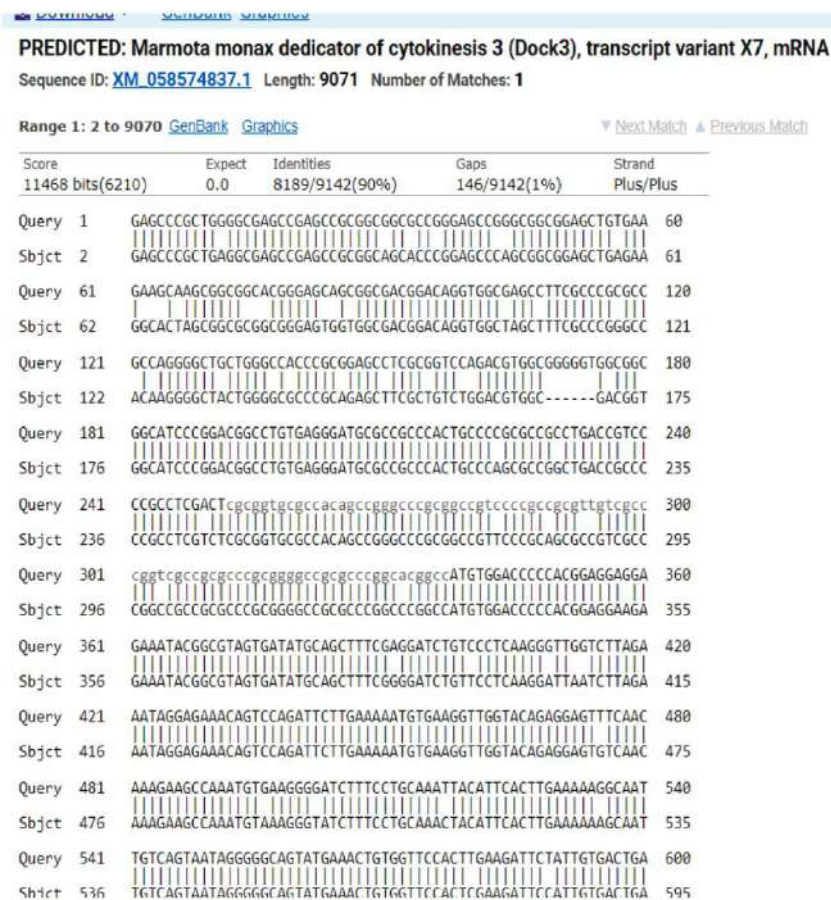


Figure S4. By acquiring the sequence of the healthy gene and comparing it to the defective gene, it was found that 10% to 20% of mutations were present in the gene.

CRISPR Sequences in Prokaryotes

Mature hsa-miR-519e-5p		Mature hsa-miR-519e-3p	
Accession	MIMAT0002829	Accession	MIMAT0002829
Description	<i>Homo sapiens</i> hsa-miR-519e-5p mature miRNA	Description	<i>Homo sapiens</i> hsa-miR-519e-3p mature miRNA
Sequence	14 - UUUCUCCAAAAGGGAGCACUUUC - 35	Sequence	52 - AAGUGCCUCCUUUUAGAGUGUU - 73
Evidence	experimental array-cloned [1]	Evidence	experimental array-cloned [1], cloned [2]

References	
1. PubMed ID: 17604727	A mammalian microRNA expression atlas based on small RNA library sequencing Landgraf P, Rusu M, Sheridan R, Sewer A, Iovino N, Aravin A, Pfeffer S, Rice A, Kamphorst AO, Landthaler M, Lin C, Sociu ND, Hermida L, Földi V, Chianelli S, Foa R, Schliwka J, Fuchs U, Novosel A, Muller RU, Schermer B, Bissels U, Inman J, Phan Q, Chien MF *Cell (2007) 129:1401-1414
2. PubMed ID: 15965474	Identification of hundreds of conserved and nonconserved human microRNAs Bentwich I, Avniel A, Karov Y, Aharonov R, Glad S, Barad O, Barzilai A, Einat P, Elinav U, Meiri E, Sharon E, Spector Y, Bentwich Z *Nat Genet (2006) 37:768-770

hsa-miR-519e is associated with one or more human diseases in the Human microRNA Disease Database [Hide](#)

[Download CSV File](#)

Show entries

Disease	Description	Category	PubMed ID
Adenocarcinoma of Lung	To be specific, lnc01833 can function as a competitive endogenous RNA (ceRNA) to adsorb miR-519e-3p through a sponge and regulate S100A4 in lung cancer, thereby being involved in LUAD progression.	lncRNA target	33173348
Stomach Neoplasms	All investigations indicated that Lnc_ASNR functioned as a ceRNA targeting miR-519e-5p and facilitated GC development by regulating the pathway of miR-519e-5p/FGFR2.	lncRNA target	34307380
Thyroid Neoplasms	Ultimately, our study revealed that MAPKAPK5-AS1 promotes proliferation and migration of thyroid cancer cells by targeting the miR-519e-5p/YWHAH axis, which provides novel insight into the development and progression of thyroid cancer.	lncRNA target	33272009
Uterine Cervical Neoplasms	Therefore, GABPB1-AS1 functioned as a tumor activator in CC pathogenesis by binding to miR-519e-5p and destroying its tumor suppressive function.	lncRNA target	32844486

Figure S5. Some human diseases are associated with miR-519e, and their corresponding accession numbers were also retrieved.

PREDICTED: Pan troglodytes complement factor H (CFH), transcript variant X1, mRNA

Sequence ID: [XM_001136531.4](#) Length: 3979 Number of Matches: 1

Range 1: 3225 to 3979 [GenBank](#) [Graphics](#) [Next Match](#) [Previous Match](#)

Score	Expect	Identities	Gaps	Strand
1266 bits(685)	0.0	732/755(97%)	1/755(0%)	Plus/Plus
Query 544	GACACTTCCTGTGTGAATCCGCCACAGTACAAAATGCTCATATACTGTGAGACAGATG	603		
Sbjct 3225	GACACTTCCTGTGTGAATCCGCCACAGTACAAAATGCTTATATAGTGTGAGACAGATG	3284		
Query 604	AGTAAATATCCATCTGGTGAGAGAGTACGTTATGAATGTAGGAGCCCTTATGAAATGTTT	663		
Sbjct 3285	AGTAAATATCCATCTGGTGAGAGAGTACGTTATCAATGTAGGAGCCCTTATGAAATGTTT	3344		
Query 664	GGGGATGAAGAGTGATGTGTTTAAATGGAACTGGACAGAACCACCTCAATGCAAGAT	723		
Sbjct 3345	GGGGATGAAGAGTGATGTGTTTAAATGGAACTGGACAGAACCACCTCAATGCAAGAT	3404		
Query 724	TCTACGGGAAAAATGTGGGCCCTCCACCTATTGACAAATGGGACATTACTTCATTCCCG	783		
Sbjct 3405	TCTACGGGAAAAATGTGGGCCCTCCACCTATTGACAAATGGGACATTACTTCATTCCCG	3464		
Query 784	TTGTCAGTATATGCTCCAGCTTCATCAGTTGAGTACCAATGCCAGAACTTGTATCAACTT	843		
Sbjct 3465	TTGTCAGTATATGCTCCAGCTTCAACAGTTGAGTACCAATGCCAGAACTTGTATGAACCTT	3524		
Query 844	GAGGGTAACAAGCGAATAACATGTAGAAATGGACAATGGTCAGAACACCAAAATGCTTA	903		
Sbjct 3525	GAGGGTAACAAGCGAATAACATGTAGAAATGGACAATGGTCAGAACACCAAAATGCTTA	3584		
Query 904	CATCCGTGTGTAATATCCCGAGAAATTATGGAAAAATTAACATAGCATTAAAGGTGGACA	963		
Sbjct 3585	CATCCGTGTGTAATATCCCGAGAAATTATGGAAAAATTAACATAGCATTAAAGGTGGAAA	3644		
Query 964	GCCAAACAGAAAGCTTTATTTGAGAACAGGTGAATCAGCTGAATTTGTGTGTAACGGGGA	1023		
Sbjct 3645	GCCAAAGAGAAAGTTATTCGAGAACAGGTGAATCAGTTGAATTTATATGTAATAATGGA	3704		
Query 1024	TATCGTCTTTTCACGTTCTCAGCATTTGCGAACACATGTTGGGATGGGAACTGGAG	1083		
Sbjct 3705	TATCGTCTTTTCACCAAGTTCTCAGCATTTGCGAACAGCATGTTGGGATGGGAACTGGAG	3764		
Query 1084	TATCCAACCTTTGTGCAAAAAGATAGAATCAATCATAAAATGCACACCTTTATTGAGAACTT	1143		
Sbjct 3765	TATCCAACCTTTGTGTAATAAAGATAGAATCAATCATAAAATGCACACCTTTATTGAGAACTT	3824		
Query 1144	TAGTATTAAATCAGTTCTTAATTTCA-TTTTAAAGTATTGTTTACTCCTTTTATTTCAT	1202		
Sbjct 3825	TAGTATTAAATCAGTTCTTAATTTCA-TTTTAAAGTATTGTTTACTCCTTTTATTTCAT	3884		
Query 1203	ACGTAAAAATTTGGATTAAATTTGTGAAAATGTAATTATAAGCTGAGACCGGTGGCTCTCT	1262		
Sbjct 3885	ATGTAAAAATTTGGATTAAATTTGTGAAAATGTAATTATAAGCTGAGACCGGTGGCTCTCT	3944		

Figure S6. Approximately 30% of the gene was found to be mutated by comparing the defective sequence with the reference gene in FASTA format.

Range 1: 1 to 1982 [GenBank](#) [Graphics](#) [▼ Next Match](#) [▲ Previous Match](#)

A. Previous Match

Related Information
[Gene](#) - associated gene details
[Genome Data Viewer](#) - aligned genomic context

Avicenna Journal of Medical Biotechnology, Vol. 17, No. 4, October-December 2025

CRISPR Sequences in Prokaryotes

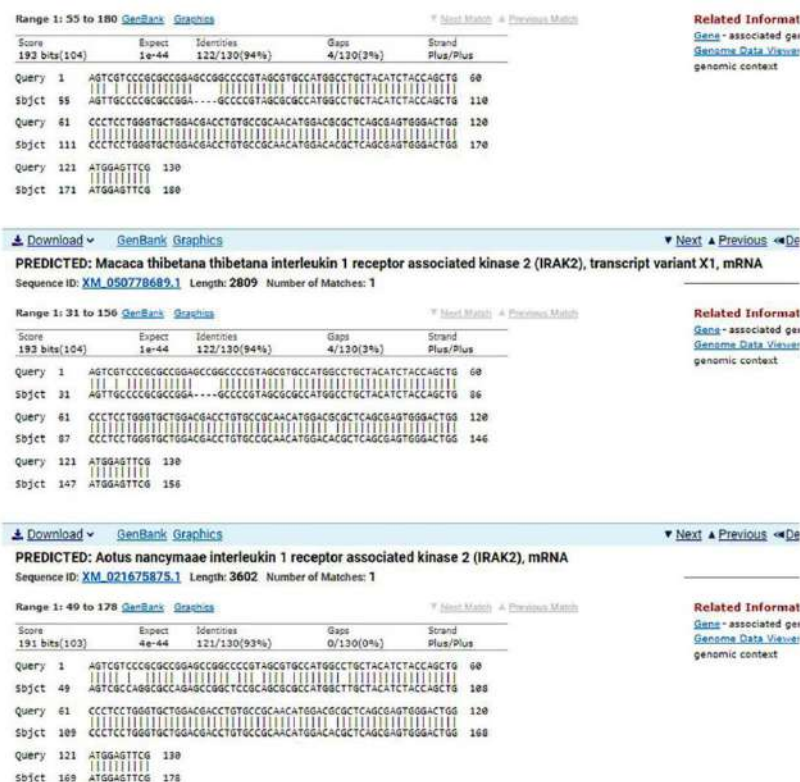


Figure S9. Analysis of the *Irak2* gene revealed 60-70% mutation frequency compared to the healthy reference, based on NCBI data. These mutations, linked to immunodeficiency, affect the interleukin-1 receptor-associated kinase 2, a key regulator of IL-1-induced NF- κ B signaling.

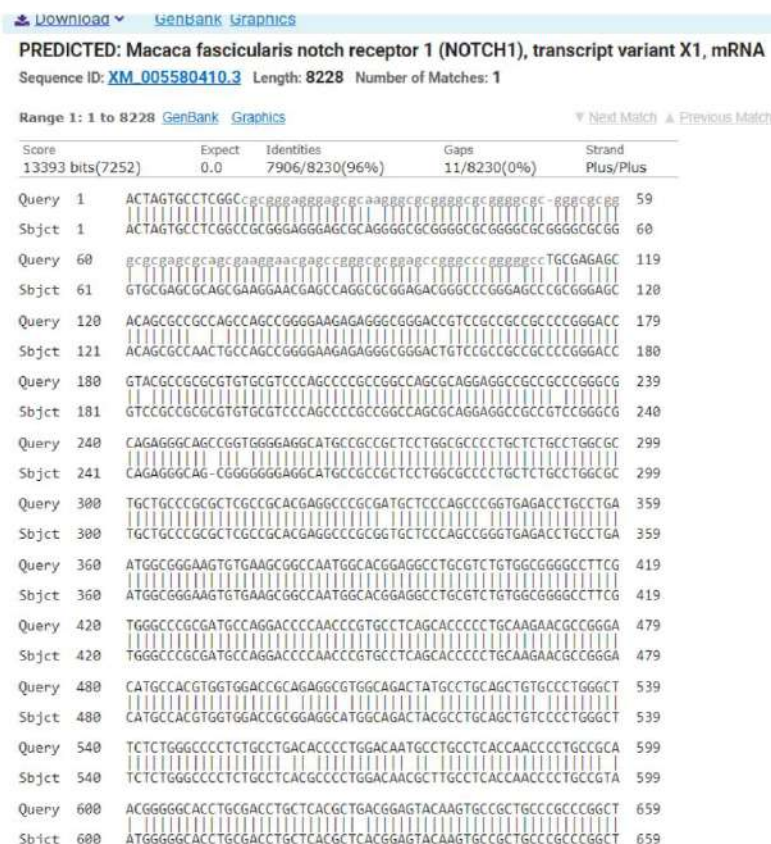


Figure S10. FASTA comparison shows ~40% mutation presence in *NOTCH1*, associated with aortic valve disease and T-cell acute lymphoblastic leukemia.

PREDICTED: Propithecus coquereli nitric oxide synthase 2, inducible (NOS2), mRNASequence ID: [XM_012648230.1](#) Length: 3462 Number of Matches: 1Range 1: 1 to 3462 [GenBank](#) [Graphics](#)[▼ Next Match](#) [▲ Previous Match](#)

Score	Expect	Identities	Gaps	Strand
4638 bits(2511)	0.0	3147/3464(91%)	4/3464(0%)	Plus/Plus
Query 265	ATGGCTGTCTTGGAAATTTCTGTTCAAGACCAAATTCACCAAGTATGCAATGAATGGG	324		
Sbjct 1	ATGGACTGTCTTGGAAATTTCTGTTCAAGACCAAATTCACCAAGTATGGCTTGAACAAG	60		
Query 325	GAAGAGACATCAACAACAATGTGGAGAAAGCCCCCTGTG-CCACCTCCAGTCCAGTGAC	383		
Sbjct 61	GAAGAGACATCAACAACAATGTGGAGAAAGCCCCCTGTGTTAACT-CAGTCCGCTGAC	119		
Query 384	ACAGGATGACCTTCAGTATCACAACCTCAGCAAGCAGCAAGTGAATGCTCCCGAGCCCCCT	443		
Sbjct 120	ACAGGATGACCTTCAGTATCACAACCTCAGCAAGCAGCAAGTGAATGCTCCCGAGCCCCCT	179		
Query 444	CGTGGAGACGGGAAAGTCTCAGAATCTCTGGTCAAGCTGGATGCAACCCATTGTG	503		
Sbjct 180	CACGGGACGGTCAAGTCTCAGAATCTCTGGTCAAGCTGGATGCAACCCATTGTG	239		
Query 504	CTCCCCACGGCATGTGAGGATCAAAAACCTGGGCGAGCGGGATGACCTTCCAAGACACACT	563		
Sbjct 240	CTGCCACAACACGTGAGATCAAAAACCTGGGCGAGTGGGACACTTCCAAGACACACT	299		
Query 564	TCACCTAAGGCCAAGGGATTTAACTTGCAGGTCCAAATCTTGCCTGGGTCATTAT	623		
Sbjct 300	CCACCAAGGCCAAGGGGCTTTCACTTGCAGGTCCAAATCTTGCCTGGGTCATTAT	359		
Query 624	GACTCCAAAAGTTTGACCAAGGACCCAGGGAACAGCCCTACCCCTCCAGTGAAGTCTCT	683		
Sbjct 360	GACCCCAAAAGTTTGACCAAGGACCCAGGGAACAGCCCTACCCCTCCAGTGAAGTCTCT	419		
Query 684	ACCTCAAGCTATCGAATTTGTCAACCAATATTACGGCTCTTCAAGAGGCAAAAATAGA	743		
Sbjct 420	ACCTCAAGCTATCGAATTTGTCAACCAATATTACGGCTCTTCAAGAGGCAAAAATAGA	479		
Query 744	GGAACTCTGGCCAGGGTGAAGCGGTAAACAAGGAGATAGAAAACAGGAACCTACCA	803		
Sbjct 480	GGAACTCTGGCCAGGGTGAAGCGGTGAAGGAGATAGAAAACAGGAACCTACCA	539		
Query 804	ACTGACGGGAGATGAGCTCATCTTGCACCAAGCAGGCTGGCGCAATGCCACAGCTG	863		
Sbjct 540	ACTGACGGGAGATGAGCTCATCTTGCACCAAGCAGGCTGGCGCAATGCCACAGCTG	599		
Query 864	CATTGGGAGGATCAGTGGTCAACCTGCAGGTCTTCGATGCCCGGAGCTGTTCCACTGC	923		
Sbjct 600	CATCGGAGGATCAGTGGTCAACCTGCAGGTCTTCGATGCCCGGAGCTGTTCCACTGC	659		
Query 924	CCGGAAATGTTTGAACACATCTGCAGACACGTGCTTACTCCACCAACATGGCAACAT	983		
Sbjct 660	CTGGGAGATGTTTGAACACATCTGCAGACACGTGCTTACTCCACCAACATGGCAACAT	719		

Figure S11. Detailed molecular analysis revealed that 16% of mutations are localized within the defective allele, providing further validation of this observation.

PREDICTED: Cebus imitator homeodomain interacting protein kinase 3 (HIPK3), transcript variant X3, mRNASequence ID: [XM_017514258.2](#) Length: 7785 Number of Matches: 1Range 1: 133 to 7785 [GenBank](#) [Graphics](#)[▼ Next Match](#) [▲ Previous Match](#)

Score	Expect	Identities	Gaps	Strand
12717 bits(6886)	0.0	7420/7669(97%)	71/7669(0%)	Plus/Plus
Query 1	GGTGGCAGCTGCCTCAGTGACGACTGCCGGCATCGCGGACCTGAGGAGATCAAGCCG	60		
Sbjct 133	GGCGGCAGCTGCCTCAGTGACGACTGCCGGCATCGCGGACCTGAGGAGATCAAGCCG	192		
Query 61	AGGCCCGCCGTCGCCACCACTCCCGCAGTCTTCTTCTCCGCTCCCGCCGGGCGTC	120		
Sbjct 193	GGGCCCGCCGTCGTCGGCACT-CCGGCTGTCTCTCTCCGGTCCCGCCGGGCGTC	251		
Query 121	AGGAATGGGCCCAATCGCCGTGGGCCCCGCACCTGCGTCCCGTAGGCCCAAGTAGC	180		
Sbjct 252	AGGAATGGGCCCAACCGCCGGGCCCCGCACCTGCGTCCCGTAGGCCCAAGTAGC	311		
Query 181	CGGAGGCCGACCGGCCCTCCCACTACCCCTCGCCCTAGCCCAAGCCGTCACCCCAAAATC	240		
Sbjct 312	TGGAGGCCGCTGGCTCCCACTACCCCTACCCCAAGCCGAGCCGTCACCCCAAAATC	371		
Query 241	CCCGGGAAGGAAGATGAGGAGACGGGCCCCGGCTTAgagccagagcagcagcagcag	300		
Sbjct 372	CCCGGGAAGGAAGATGAGGAGACGGGCCCCGGCTTAgagccagagcagcagcagcag	431		
Query 301	cagcagcGGTGGGGGAGGGTGTTCGCCGTTTCTCTCAGCCGCCAGGACAAGATGGCA	360		
Sbjct 432	CAGCAGCGGTGGGGGAGGGTGTTCGCCGTTTCTCTCAGCCGCCAGGACAAGATGGCA	491		
Query 361	GCGGCCGCGGAGAGGGGCTGAGCCCGGGCTGGTGGTGGCGCTGCTGAAGCGCTGGCT	420		
Sbjct 492	GCGGCCGCGGAGAGGGGCTGAGCCCTGGGCTGGTGGTGGCGCTGCTGAAGCGCTGGCT	551		
Query 421	CCCGTCCCGGCACGGCCCTGCGCCCAACCCGGACATGCTAGGGCTGCGGCCGCCCG	480		
Sbjct 552	CCCTGTCCCGGCACGGCCCTGCGCCCAACCCGGACATGCTAGGGCTGCGGCCGCCCG	611		
Query 481	AAGAGGAGAGAGCGCGGCCCTTAGGAAGGTATGGCTCACAAGTCTTGGTACCCACC	540		
Sbjct 612	AAGAGGAGAGAGCGCGGCCCTTAGGAAGGTATGGCTCACAAGTCTTGGTACCCACC	671		
Query 541	ATATGTTTATCAAACTCAGTCAAGTGCCCTTTTGTAGTGTGAAGAACTCAAGTAGAGCC	600		
Sbjct 672	ATATGTTTATCAAACTCAGTCAAGTGCCCTTTTGTAGTGTGAAGAACTCAAGTAGAGCC	731		
Query 601	AAGCAGTTGTGTATTCCAGGAAGAACTATCCACGGACCTATGTGAATGGTAGAACTT	660		
Sbjct 732	AAGCAGTTGTGTATTCCAGGAAGAACTATCCACGGACCTATGTGAATGGTAGAACTT	791		

Figure S12. Comparative analysis of the FASTA sequences of the healthy and mutated *Hipk3* genes revealed that approximately 20% of the total observed variations are found in the mutated sequence.

CRISPR Sequences in Prokaryotes

PREDICTED: Pongo abelii NUMB endocytic adaptor protein (NUMB), transcript variant X10, mRNA
Sequence ID: [XM_054529722.1](#) Length: 4233 Number of Matches: 1

Range 1: 694 to 4233 [GenBank](#) [Graphics](#)

[Next Match](#) [Previous Match](#)

Score	Expect	Identities	Gaps	Strand
6220 bits(3368)	0.0	3491/3550(98%)	10/3550(0%)	Plus/Plus
Query 55	ATTTGAGGCTTAAGCAACTTCTTCGGGGAAAGAGTGGCAGTGCAGCCACTGTTACAAATTC	114		
Sbjct 694	ATTTGAGGCTTAAGCAACTTCTTCGGGGAAAGAGTGGCAGTGCAGCCACTGTTGCAATTC	753		
Query 115	AAGATCTTGATCTATATCCATAGATTGGAATATTGGTGGCCAGCAATCTCAGACGCCT	174		
Sbjct 754	AAGATCTTGATCTATATCCATAGATTGGAATATTGGTGGCCAGCAATCTCAGACACCT	813		
Query 175	CACCTAGGACAAATGAGGAACTGAGGCTTGGTGAAGTTACGAAACTTGTCCAAAATCAC	234		
Sbjct 814	CACCTAGGACAGATGAGGAACTGAGGCTTGGTGAAGTTACGAAACTTGTCCAAAATCAC	873		
Query 235	ACAACCTTGTAAGGGCACAGCCAAGATTCAGAGCCAGGCTGTAAAAATAAAAATGAACAA	294		
Sbjct 874	ACAACCTTGTAAGGGCACAGCCAAGATTCAGAGCCAGGCTGTAAAAATAAAAATGAACAA	933		
Query 295	ATTACGGCAAAGTTTATAGGAGAAAGAGGATGTTTATGTTCCAGAGGCCAGTCGTCACA	354		
Sbjct 934	ACTACGGCAAAGTTTATAGGAGAAAGAGGATGTTTATGTTCCAGAGGCCAGTCGTCACA	993		
Query 355	TCAGTGGCAGACAGATGAAGAAGCGTTCCACCGGAAATGTAGCTTCCCGGTTAAGTA	414		
Sbjct 994	TCAGTGGCAGACAGATGAAGAAGCGTTCCACCGGAAATGTAGCTTCCCGGTTAAGTA	1053		
Query 415	CCTTGGCCATGTAGAAGTTGATGAATCAAGAGGAATGCACATCTGTGAAGATGCTGTAAA	474		
Sbjct 1054	CCTTGGCCATGTAGAAGTTGATGAATCAAGAGGAATGCACATCTGTGAAGATGCTGTAAA	1113		
Query 475	AAGATTGAAAGCTGAAAGGAAGTTCTTCAAAGGCTCTTTGGAAAAACTGGAAAGAAAGC	534		
Sbjct 1114	AAGATTGAAAGCTGAAAGGAAGTTCTTCAAAGGCTCTTTGGAAAAACTGGAAAGAAAGC	1173		
Query 535	AGTTAAAGCAGTTCTGTGGGTCACGAGATGGACTCAGAGTTGTGGATGAAAAAATAA	594		
Sbjct 1174	TGTTAAAGCAGTTCTGTGGGTCACGAGATGGACTCAGAGTTGTGGATGAAAAAATAA	1233		
Query 595	GGACCTCATAGTTGACACAGATAGAGAAAGTTCTTTCTGTGCCCCAGACAGGAACCT	654		
Sbjct 1234	GGACCTCATAGTTGACACAGATAGAGAAAGTTCTTTCTGTGCCCCAGATAGGAACCT	1293		
Query 655	TGATAGAGCCTTTTCTTACATATGCCGTGATGGCACCACCTCGTCGCTGGATCTGTCACTG	714		
Sbjct 1294	TGATAGAGCCTTTTCTTACATATGCTGATGGCACCACCTCGTCGCTGGATCTGTCACTG	1353		

Figure S13. FASTA comparison demonstrates ~30% of mutations in the defective gene, with additional *Numb* gene mutations identified via BLAST analysis on the NCBI server.